



ELSEVIER

Available online at [www.sciencedirect.com](http://www.sciencedirect.com)

SCIENCE @ DIRECT®

Ocean Engineering 32 (2005) 1486–1502

OCEAN  
ENGINEERING

[www.elsevier.com/locate/oceaneng](http://www.elsevier.com/locate/oceaneng)

# The nonlinear hydrodynamic model for simulating a ship steering in waves with autopilot system

Ming-Chung Fang\*, Jhih-Hong Luo

*Department of Systems and Naval Mechatronic Engineering, National Cheng Kung University,  
Tainan 701, Taiwan, ROC*

Received 24 June 2004; accepted 27 September 2004

Available online 11 March 2005

---

## Abstract

In the paper, a hydrodynamic numerical model including wave effect is developed to simulate ship autopilot systems by using the time domain analysis. The PD controller and the sliding mode controller are adopted as the autopilot systems. The differences of simulation results between two controllers are analyzed by cost function composed of heading angle error and rudder deflection, either in calm water or in waves. The results in calm water show that both controllers are tracking well for the desired route with the similar cost function value by tuning the key design parameters. However, the course tracking ability of the controller using sliding mode in waves is generally better even the cost function value is similar.

© 2005 Elsevier Ltd. All rights reserved.

*Keywords:* Hydrodynamic; Control; Wave; Autopilot

---

## 1. Introduction

When the ship sails in the seaway, the autopilot system is usually applied to make the ship navigate in the commanded course by automatically altering the deflection of the rudder. In past years, many literatures only investigate the autopilot ability in calm water and assume external factors (e.g. waves) are enabled to overcome. However, some external factor especially the wave may play an important role in the ship maneuvering characteristics. Practically the ship always sails in waves and will behave differently

---

\* Corresponding author. Tel.: +886-6-274-7018 ext.211; fax: +886-6-208-0592.

E-mail address: [fangmc@mail.ncku.edu.tw](mailto:fangmc@mail.ncku.edu.tw) (M.-C. Fang).

from that in calm water because ship motion due to the wave effect is significant. Therefore, the wave effect on the ship course tracking ability must be taken into consideration. The mathematical model for predicting a ship maneuvering in calm water was early developed by many authors, e.g. Hirano (1980) and Inoue et al. (1981a,b). Some valuable information for naval architects has been found. However, if the wave effect can be included in the mathematical model, the prediction will be more reliable.

In order to simulate the ship maneuvering in waves, the compact mathematical model must include the hydrodynamic effects from seakeeping and maneuvering of the ship. Some simplified mathematical models for predicting the maneuvering of a ship in waves have already been developed by several authors. Hamamoto and Kim (1993) and Hamamoto et al. (1994) used the six degrees of freedom model combining maneuvering and seakeeping to simulate the turning circle and zig-zag trial of a ship sailing in waves, the surf-riding phenomenon and directional stability were also investigated. Recently Bailey (1999) proposed a unified mathematical model including maneuvering and seakeeping to simulate the ship steering behavior in waves. The most important point in his mathematical model is considering the relationship between maneuvering derivatives and seakeeping coefficients with encounter frequency variations. Although this model seems more rigorous, it is very complicated due to the coupling effect of maneuvering derivatives and seakeeping coefficients. Munif and Umeda (2000) predicted the roll motion and capsizing of a moderate-speed in astern waves by a modular-type maneuvering mathematical model including heave and pitch effects. Their results show that the effect of heave and pitch motions on the ship maneuvering can be significant when the wave steepness becomes larger. Umeda and Hashimoto (2002) utilized a four degrees of freedom numerical model with dense grids of control parameters and the sudden-change concept to intensively explore nonlinear ship motions in following and quartering seas. This model can successfully explain the capsizing phenomena qualitatively, but overestimates the danger of capsizing quantitatively.

The PD controller with fixed design parameters is a conventional autopilot system for ship steering. Such controller can be made to work well for particular operating conditions, but its performance will become weak if these conditions vary. The reason is ship dynamics change with the ship velocity, loading and external disturbances, i.e. wave, wind, current, etc. Manual adjustments of the design parameters are necessary in several cases. Therefore, many literatures devote to improve this type controller or propose substitutions. Nejim (2000) proposed a limited authority adaptive PD controller to automatically adjust the design parameters. The simulation results presented that limited authority adaptive control where only part of the controller structure is allowed to vary can reduce the complexity of adaptive controller. Tzeng and Lin (2000) proposed internal model control based adaptive ship steering autopilot, which is characterized by a model-based design approach that provides explicit structure connections between the controller and the ship model. Once the ship model parameters are estimated immediately, the controller parameters are adjusted accordingly to adopt different operating conditions. Sliding mode controller is also frequently adopted in automating steering (Slotine and Li, 1991; Healey and Lienard, 1993; Fossen, 1994; McGoekin et al., 2000a,b) and known to provide good performance robustness. This type controller is based on switching control that provides additional control action when the dynamics of the system vary due to nonlinearities.

In the paper, an improved nonlinear hydrodynamic model with six degrees of freedom is developed and the PD controller and the sliding mode controller are adopted to analyze the autopilot ability of the ship when it is automatically steering in waves. The autopilot ability in calm water and regular waves is tested by a commanded course made up of several waypoints. The cost function composed of heading angle error and rudder deflection is used to judge the performance of the controllers. The wave effect on the simulation is also checked by the cost function.

### 2. Mathematical model

Three coordinate systems are used to describe the present mathematical model and shown in Fig. 1. The coordinate system  $O-X_0Y_0Z_0$  describing the incident wave is fixed on the calm water surface. The  $X_0$  coordinate and the wave direction are parallel. The body coordinate system  $G-xyz$  with its origin at the ship's center of gravity is moving with the ship motion. The horizontal body coordinate system  $G-x'y'z'$  is also fixed at the ship's center of gravity, but  $Gx'y'$  plane is always parallel to  $OX_0Y_0$  plane.

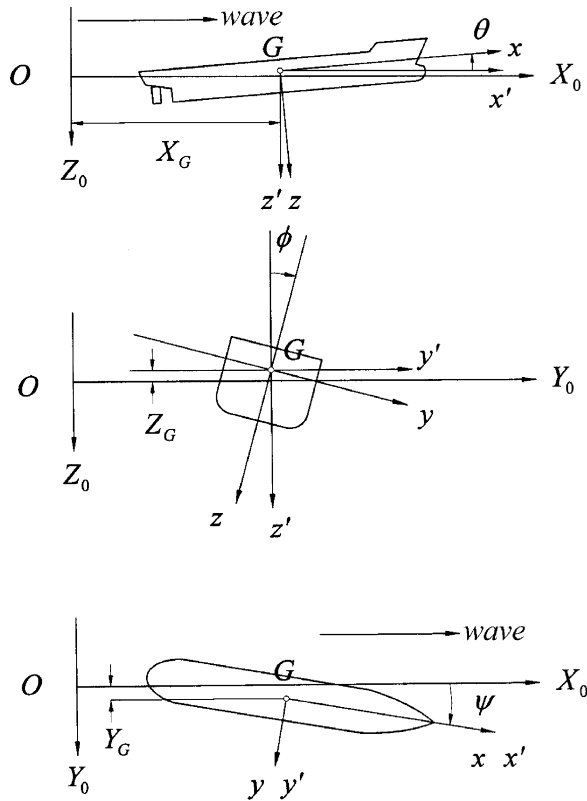


Fig. 1. Coordinate system.

The horizontal body coordinate system is used to describe equations of motions and the corresponding forces. Based on the mathematical model used by Hamamoto and Kim (1993) and Hamamoto et al. (1994), an extensive nonlinear model combining maneuvering and seakeeping for the ship moving in waves and the engine torque equation are used simultaneously in this study and stated as below,

$$\text{Surge : } m(\dot{u} - v\dot{\psi}) = (m_y - X_{v\dot{\psi}})v\dot{\psi} - m_x\dot{u} - m_z w\dot{\theta} + X_{FK} + X_{RF} + T(1 - t_p) - R \quad (1)$$

$$\begin{aligned} \text{Sway : } & m(\dot{v} + u\dot{\psi}) \\ &= -m_x u\dot{\psi} - m_y \dot{v} - Y_v v - Y_{\dot{\psi}} \dot{\psi} + Y_{\dot{\psi}} \dot{\psi} + Y_{|v|} |v| + Y_{|v|\dot{\psi}} |v|\dot{\psi} \\ &+ Y_{\dot{\psi}|v|} \dot{\psi}|v| + Y_{FK} + Y_{DF} + Y_{RF} \end{aligned} \quad (2)$$

$$\text{Heave : } m\dot{w} = -m_z \dot{w} - Z_w w - Z_{\dot{\theta}} \dot{\theta} - Z_{\theta} \dot{\theta} - Z_{\theta} \theta + Z_{FK} + Z_{DF} + mg \quad (3)$$

$$\begin{aligned} \text{Roll : } & I_{xx} \ddot{\phi} - I_{xx} \dot{\theta} \dot{\psi} \\ &= J_{xx} \dot{\theta} \dot{\psi} - J_{xx} \ddot{\phi} - K_{\phi} \dot{\phi} + (Y_v v - Y_{\dot{\psi}} \dot{\psi}) z_G + K_{FK} + K_{DF} + K_{RF} \end{aligned} \quad (4)$$

$$\begin{aligned} \text{Pitch : } & I_{yy} \ddot{\theta} + I_{xx} \dot{\psi} \dot{\phi} \\ &= -J_{xx} \dot{\phi} \dot{\psi} - J_{yy} \ddot{\theta} - M_{\dot{\theta}} \dot{\theta} - M_{\theta} \theta - M_{\dot{w}} \dot{w} - M_w w + M_{FK} + M_{DF} \end{aligned} \quad (5)$$

$$\begin{aligned} \text{Yaw : } & I_{zz} \ddot{\psi} - I_{xx} \dot{\theta} \dot{\phi} \\ &= J_{xx} \dot{\theta} \dot{\phi} - J_{zz} \ddot{\psi} - N_v \dot{v} - N_v v - N_{\dot{\psi}} \dot{\psi} + N_{\dot{\psi}|v|} \dot{\psi}|v| + N_{v\dot{\psi}} v^2 \dot{\psi} + N_{v\dot{\psi}} v \dot{\psi}^2 \\ &+ N_{\phi} \dot{\phi} + N_{|v|\phi} |v|\dot{\phi} + N_{\dot{\psi}|\phi|} \dot{\psi}|\dot{\phi}| + (-Y_v v + Y_{\dot{\psi}} \dot{\psi} + Y_{|v|} |v|) \\ &+ Y_{|v|\dot{\psi}} |v|\dot{\psi} + Y_{\dot{\psi}|v|} \dot{\psi}|v|) x_G + N_{FK} + N_{DF} + N_{RF} \end{aligned} \quad (6)$$

$$\text{Engine : } 2\pi I_{pp} \dot{n} = Q_E + Q_P \quad (7)$$

where  $m$  and  $I$  are ship mass and mass moment of inertia, respectively. Surge, sway and heave velocities are represented by  $u$ ,  $v$  and  $w$ , respectively, whereas roll, pitch and yaw displacements are represented by  $\phi$ ,  $\theta$ , and  $\psi$ , respectively.  $T$  is propeller thrust,  $R$  is ship resistance,  $t_p$  is the thrust deduction coefficient, and  $g$  is gravitational acceleration. In Eqs. (3) and (5), the corresponding hydrodynamic coefficients with respect to heave and pitch can be referred to Kim et al. (1980), which can be calculated by Frank close-fit method. The  $(m_y - X_{v\dot{\psi}})$  term can be written as  $C_m m_y$ , and  $C_m$  is about 0.5–0.75 (Yoshimura and Nomoto, 1978).  $m_x$ ,  $m_y$  and  $m_z$  represent the added masses with respect to  $x$ ,  $y$  and  $z$  axes, respectively, whereas  $J_{xx}$ ,  $J_{yy}$  and  $J_{zz}$  represent the added moments of inertia with respect to  $x$ ,  $y$  and  $z$  axes, respectively. The linear maneuvering derivatives of

sway and yaw motions in still water can be estimated by empirical formulas (Inoue et al., 1981a,b). The roll damping coefficient  $K_{\dot{\phi}}$  can be computed from the empirical formula derived by Takahashi (1969). The corresponding nonlinear terms for maneuvering derivatives can be referred to Hirano and Takashina (1980) and Inoue et al. (1981a,b). The terms  $I_{PP}$ ,  $Q_E$ ,  $Q_P$ ,  $n$  in Eq. (7) represent the moment of inertia of propeller-shafting system, the propeller torque, the main engine torque, and the revolutions per minute of propeller, respectively.  $x_G$  and  $z_G$  are  $x$ - and  $z$ - coordinates of the point which lateral force acts, respectively. Subscripts FK, DF, RF represent Froude–Krylov forces, diffraction forces, and rudder forces (Hirano, 1980), respectively.

According to the Froude–Krylov hypothesis, the wave shape is assumed not to be destroyed with the existence of ship hull. The formula of the regular wave used in this paper is expressed as

$$\zeta_w = a \cos k(X_0 - ct) \quad (8)$$

where  $k$  is wave number,  $c$  is wave celerity,  $t$  is time, and  $a$  is wave amplitude. When the pressure gradient corresponding to horizontal body coordinate system is obtained, the incident wave forces and moments can be expressed by using Gauss's theorem considering the instant relative position between ship and wave.

$$X_{FK} \cong -\rho g \cos \psi \int_L F(x)A(x) \sin k(X_G + x \cos \psi - ct) dx \quad (9)$$

$$Y_{FK} \cong \rho g \sin \psi \int_L F(x)A(x) \sin k(X_G + x \cos \psi - ct) dx \quad (10)$$

$$Z_{FK} \cong -\rho g \int_L A(x)dx - \rho g \int_L F(x)A(x) \cos k(X_G + x \cos \psi - ct) dx \quad (11)$$

$$K_{FK} \cong -\rho g \int_L y'_B(x)A(x)dx - \rho g \sin \psi \int_L F(x)A(x)z'_B(x) \sin k(X_G + x \cos \psi - ct) dx \quad (12)$$

$$M_{FK} \cong \rho g \int_L A(x)x dx + \rho g \int_L F(x)A(x)x \cos k(X_G + x \cos \psi - ct) dx \quad (13)$$

$$N_{FK} \cong \rho g \sin \psi \int_L F(x)A(x)x \sin k(X_G + x \cos \psi - ct) dx \quad (14)$$

where

$$F(x) = ak \frac{\sin\left(k \frac{\bar{B}(x)}{2} \sin \psi\right)}{k \frac{\bar{B}(x)}{2} \sin \psi} \exp\left[-k\left(Z_G - x\theta + \frac{A(x)}{\bar{B}(x)}\right)\right] \quad (15)$$

$A(x)$  is the wetted area of each hull strip at each instant of time.  $y'_B(x)$  and  $z'_B(x)$  are the coordinate of centroid of the instant wetted hull strip.  $\rho$  is density of water and  $\bar{B}(x)$  is the breadth of each strip.

The diffraction forces and moments are also done with a linear strip theory, therefore, the wave diffraction for surge,  $X_{DF}$ , cannot be calculated. However, it is generally small due to the slenderness of the ship and can be neglected.

$$Y_{DF} = \int_L \left[ \bar{m}_{SS}(x) \frac{d}{dt} \dot{w}_H(x) + \bar{N}_{SS}(x) \dot{w}_H(x) \right] dx \tag{16}$$

$$Z_{DF} = \int_L \left[ \bar{m}_{HH}(x) \frac{d}{dt} \dot{w}_V(x) + \bar{N}_{HH}(x) \dot{w}_V(x) \right] dx \tag{17}$$

$$K_{DF} = \int_L \left[ \bar{m}_{RR}(x) \frac{d}{dt} \dot{w}_R(x) + \bar{N}_{RR}(x) \dot{w}_R(x) \right] dx \tag{18}$$

$$M_{DF} = \int_L \left[ \bar{m}_{HH}(x) \frac{d}{dt} \dot{w}_V(x) + \bar{N}_{HH}(x) \dot{w}_V(x) \right] (-x) dx \tag{19}$$

$$N_{DF} = \int_L \left[ \bar{m}_{SS}(x) \frac{d}{dt} \dot{w}_H(x) + \bar{N}_{SS}(x) \dot{w}_H(x) \right] x dx \tag{20}$$

where  $\bar{m}_{ij}(x)$  and  $\bar{N}_{ij}(x)$  represent the added mass and wave damping of each strip in  $i$  direction caused by  $j$  motion ( $i, j = S$  for sway, H for heave, R for roll).  $\dot{w}_H(x)$  and  $\dot{w}_V(x)$  represent the average wave velocity at each strip in horizontal and vertical directions, respectively.  $\dot{w}_R(x)$  is the average variation rate of the wave slope. The following improved formulas for calculating  $\dot{w}_H(x)$ ,  $\dot{w}_V(x)$  and  $\dot{w}_R(x)$  are used in Eqs. (16)–(20),

$$\begin{aligned} \dot{w}_H(x) = & akc \sin \psi \exp[-k(Z_G - x\theta + z'_B(x))] \times \cos k(X_G + x \cos \psi \\ & - y'_B(x) \sin \psi - ct) \end{aligned} \tag{21}$$

$$\dot{w}_V(x) = akc \exp[-k(Z_G - x\theta + z'_B(x))] \times \sin k(X_G + x \cos \psi - y'_B(x) \sin \psi - ct) \tag{22}$$

$$\begin{aligned} \dot{w}_R(x) = & -ak^2c \sin \psi \exp[-k(Z_G - x\theta + z'_B(x))] \times \cos k(X_G + x \cos \psi \\ & - y'_B(x) \sin \psi - ct) \end{aligned} \tag{23}$$

### 3. Control systems for ship course tracking

In this section, the autopilot control systems are incorporated with Eqs. (1)–(7) to simulate the ship course tracking which is composed of several waypoints. A line-of-sight

guidance (Healey and Lienard, 1993; McGookin et al., 2000a,b) is introduced to guide the ship to sail to commanded waypoints. The desired ship-heading angle directed to the current waypoint position is calculated by the following formula.

$$\psi_d = \tan^{-1} \left( \frac{y_{wp} - y_p}{x_{wp} - x_p} \right) \quad (24)$$

where  $(x_p, y_p)$  is the coordinate of the instantaneous ship position whereas  $(x_{wp}, y_{wp})$  is the coordinate of the waypoint position. Each waypoint has its own acceptable radius that is typically around one to three ship lengths. If the distance between the ship position and waypoint is smaller than this acceptable radius, next waypoint will be acquired to guide the ship to sail to next position.

As mentioned before, two control systems are adopted to execute the course tracking by altering the rudder deflection. One is PD controller (Munif and Umeda, 2000; Nejm, 2000) and the other is the sliding mode controller (Slotine and Li, 1991; Healey and Lienard, 1993; Fossen, 1994; McGookin et al., 2000a,b). The PD controller is the most widely used among many autopilot systems because of its simplicity, which deflects the rudder angle according to the heading error and yaw rate and can be expressed in the following equation.

$$\delta = -\bar{a}(\psi - \psi_d) - \bar{b}\dot{\psi} \quad (25)$$

where  $\bar{a}$  is yaw gain,  $\bar{b}$  is yaw rate gain and  $\delta$  is the required rudder angle.

The sliding mode controller is also often applied because of its good performance robustness. This control theory has a switching action, which provides a robustness to match uncertainties. Since the rudder angle is the only input being controlled in the present study, a single-input-multiple-states model (Healey and Lienard, 1993; Fossen, 1994) is linearized from Eqs. (2) and (6) and can be derived as below,

$$(m + m_y)\dot{v} + Y_{\dot{v}}\dot{r} = -Y_v v + Y_{\dot{v}} r + Y_{\delta}\delta \quad (26)$$

$$N_{\dot{v}}\dot{v} + (I_{zz} + J_{zz})\dot{r} = (-N_v - Y_v x_G)v + (-N_{\dot{v}} + Y_{\dot{v}} x_G)r + N_{\delta}\delta \quad (27)$$

$$\dot{\psi} = r \quad (28)$$

In this study, the effect of  $x_G$  which Hamamoto et al. neglected in Eq. (6) has been included to correct the rudder control accuracy because the maneuvering derivatives are calculated with respect to midship (Inoue et al., 1981a,b). Replacing Eqs. (26)–(28) by the matrix form and multiplying the inverse mass matrix to each side of the equation, the single-input-multiple-states model can be transferred into the following form,

$$\begin{bmatrix} \dot{v} \\ \dot{r} \\ \dot{\psi} \end{bmatrix} = \begin{bmatrix} a_{11} & a_{12} & 0 \\ a_{21} & a_{22} & 0 \\ 0 & 1 & 0 \end{bmatrix} \begin{bmatrix} v \\ r \\ \psi \end{bmatrix} + \begin{bmatrix} b_1 \\ b_2 \\ 0 \end{bmatrix} \delta \quad (29)$$

or simply as

$$\dot{x}_h = A_h x_h + b_h \delta \tag{30}$$

It is practical to specify the desired sway velocity as zero during steering. Therefore, the sliding surface  $\sigma_h$  is defined as

$$\sigma_h = h_1 v + h_2 (r - r_d) + h_3 (\psi - \psi_d) \tag{31}$$

where  $h_i$  ( $i = 1, 2, 3$ ) are the components of right eigenvector  $\mathbf{h}$  and  $r_d$  is the desired yaw rate. In order to stabilize the sway-yaw dynamics, we choose  $\mathbf{k} = [k_1, k_2, 0]^T$  such that:

$$A_C = A_h - b_h \mathbf{k}^T = \begin{bmatrix} a_{11} - b_1 k_1 & a_{12} - b_1 k_2 & 0 \\ a_{21} - b_2 k_1 & a_{22} - b_2 k_2 & 0 \\ 0 & 1 & 0 \end{bmatrix} \tag{32}$$

Hence, two of the closed-loop eigenvalues  $\lambda_1$  and  $\lambda_2$  will simply be given to solve  $k_1$  and  $k_2$ . Once  $A_C$  is decided, right eigenvector  $\mathbf{h}$  can be solved from  $A_C^T \mathbf{h} = 0$  corresponding to  $\lambda_3 = 0$ . Then the sliding mode control law for  $\delta$  becomes

$$\delta = -\mathbf{k}^T x_h + (\mathbf{h}^T b_h)^{-1} \left[ \mathbf{h}^T \dot{x}_{hd} - \eta_h \tanh\left(\frac{\sigma_h}{\phi_h}\right) \right] \tag{33}$$

where  $\dot{x}_{hd}$  is the desired state vector,  $\eta_h$  is switching gain and  $\phi_h$  is the boundary layer thickness.

From the Eqs. (25) and (33), we can see the difference between two controllers. The rudder angle required in PD controller is calculated only by heading error and yaw rate. However, the required rudder deflection for sliding mode controller has to be determined by sway velocity, heading error, yaw rate, desired yaw acceleration and desired yaw rate, which can be investigated in detail from Eqs. (29), (31), (32) and (33).

In order to understand the quality of operation with respect to the corresponding controller, the cost function (McGookin et al., 2000a,b) is used as the judgment, which is defined by the following equation,

$$C_{\text{total}} = \left[ \sum_{i=0}^N (\sigma(\Delta\psi_i)^2 + \delta_i) \right] + \left[ P |n_{wp} - n_{\text{max}}| \right] \tag{34}$$

The first term of the right-hand side of the Eq. (34) is related to the course changing, in which  $N$  is the total number of iterations in the time simulation process,  $\sigma$  is a weighting factor,  $\Delta\psi_i$  is the  $i$ th heading error between desired heading and actual heading, and  $\delta_i$  is the  $i$ th rudder angle. The main function of the weighting factor,  $\sigma$ , is to amplify the heading error component to be the same order as the rudder component. It is obvious that the heading error component and rudder deflection component are mutually dependent on each other, therefore their magnitude had better be the same order. Without external disturbances, decreasing the heading error will increase the rudder deflection, and conversely decreasing the rudder deflection will increase the heading error. The second term of the right-hand side of the Eq. (34) is related to the track keeping and used as

a penalty if the autopilot system misses the set waypoint, in which  $P$  is an arbitrary large value to penalize the cost and is taken as a value 10000 in this study.  $n_{wp}$  is the number of passing waypoints acquired by the autopilot and  $n_{max}$  is the maximum number of waypoints that should be acquired.

#### 4. Results and discussion

In this paper, the investigation is focused on the simulation of different ship autopilot control systems in waves. Firstly the ship sailing course must be decided. Here a commanded course composed of three waypoints is chosen, and each acceptance radius is assumed to be double of ship length. A container ship is selected for numerical calculation in this study, its initial velocity is 11.97 m/s, the maximum rudder deflection is  $35^\circ$  and the rate limit is set to be  $2.5^\circ/s$ . The principal particulars of the container ship are listed in Table 1. For simplification, the water depth is assumed to be infinitely deep. Then, using the trial and error method, the key design parameters in both systems, PD controller and sliding mode controller, can be tuned to proper values to make the cost function value in calm water be similar and approximately optimal. For PD controller, only two parameters, yaw gain ( $\bar{a}$ ) and yaw rate gain ( $\bar{b}$ ), must be decided. However, four parameters are needed to be tuned for sliding mode controller. Two parameters ( $\lambda_1, \lambda_2$ ) are eigenvalues of the closed loop system whereas the other two are switching gain and boundary layer thickness. These eigenvalues of the closed loop system are used to calculate the feedback gain vector  $\mathbf{k}$  and right eigenvector  $\mathbf{h}$ . The 4th order Runge–Kutta numerical integration method is adopted here for the time domain simulation and then the corresponding cost function

Table 1  
The principal particulars of the container ship

Length (m)	185.5
Breadth (m)	30.2
Depth (m)	16.6
Draft (m)	5.9
Trim (aft) (m)	4.2
Metacentric height (m)	6.66
Displacement volume ( $m^3$ )	18700
Block coefficient	0.5772
Prismatic coefficient	0.602
Waterline coefficient	0.7101
<i>Propeller</i>	
Propeller diameter (m)	7.45
Propeller pitch (m)	7.45
Thrust deduction coefficient	0.1769
Effective propeller wake coefficient	0.222
<i>Rudder</i>	
Rudder height (m)	8.4
Area ( $m^2$ )	40.42
Aspect ratio of rudder	1.55

values can be acquired with the known parameters stated above. In the present study, the yaw gain and yaw rate gain of the PD controller are taken as the values 0.17 and 0.7, respectively. For sliding mode controller, the values of first closed loop eigenvalue, second close loop eigenvalue, switch gain, and boundary layer thickness are set to be  $-0.1$ ,  $-0.2$ , 0.04, and 0.5, respectively. The time simulation accuracy in Runge–Kutta integration method is affected by time step. According to the investigation, the simulation results with time step 0.05 s or less is almost the same as that with 0.1 s, but the time for simulation is more and will delay the simulation speed. On the other hand, if the time step increases to 0.2 s or more, the simulation will lose the reality and the phenomenon of aliasing will be found. Therefore, after the investigation, the appropriate time interval of the numerical integration for the present real time simulation is set to be 0.1 s here. The wave length to ship length ( $\lambda/L$ ) is set to be 1 and the wave height is 3 m.

In order to see the wave effect on the simulation, the situation in calm water is investigated firstly. The time simulation of the ship trajectories in calm water using both controllers is shown in Fig. 2. During the time duration of simulation, it is assumed that the maximum number of waypoints can be acquired is  $n_{\max} = 3$ . The solid line represents PD controller response and the dash line represents sliding mode controller response. It can be seen both trajectories are similar and pass through the acceptance regions of all waypoints. The cost function values are presented in Table 2, which indicates that the value of the sliding mode controller is slightly larger than that of the PD controller under the same simulation time. The amount of the rudder deflection in PD controller is larger than that in sliding mode controller whereas the result of heading error amount is contrary. This phenomenon indicates that the relationship between heading tracking accuracy and rudder deflection usage is conflicting. The time histories for different mode of ship motion

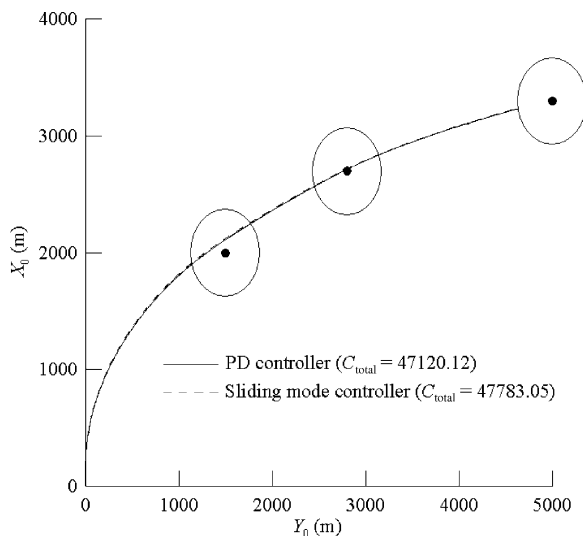


Fig. 2. The time domain simulation of ship trajectories in calm water.

Table 2  
Cost function value (in calm water)

	Cost due to heading error	Cost due to rudder deflection	Total cost
PD controller	23251.36	23868.76	47120.12
Sliding mode controller	24363.49	23419.56	47783.05

response are shown in Figs. 3 and 4 for reference. In figures,  $\zeta$  expresses the heave displacement. The rudder deflections for both control systems are controlled less than  $10^\circ$ . The results show no motion response for heave mode, and the pitch angle with initial trim almost keeps constant. The amplitudes of sway velocity ( $v$ ) and roll motion ( $\phi$ ) change slightly with rudder deflections. Consequently, the additional resistance on the surge motion is small and does not significantly affect the surge velocity ( $u$ ).

Fig. 5 shows the time simulation results in regular waves, in which the key design parameters for both controllers are kept unchanged. In this case, the container ship is

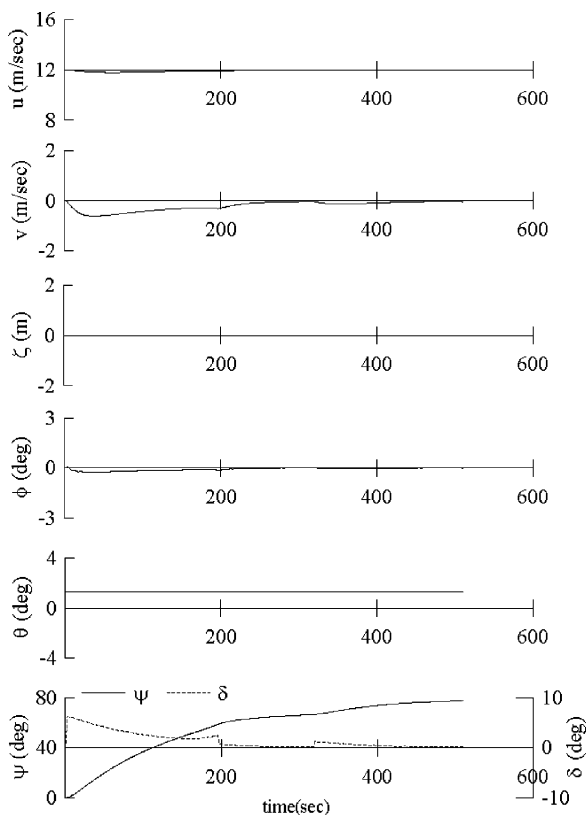


Fig. 3. The motion response for PD controller in calm water.

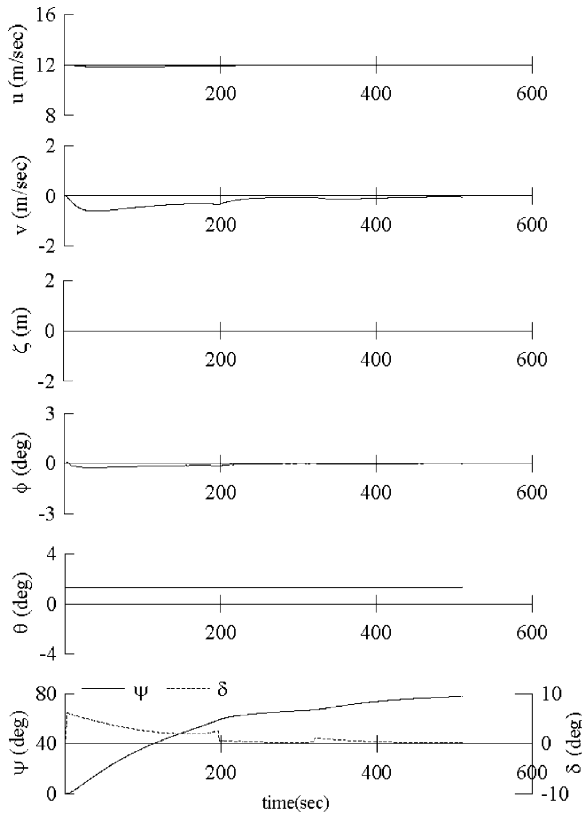


Fig. 4. The motion response for sliding mode controller in calm water.

assumed to be initially in following waves with 3 m wave heights, and the wave length is equal to the ship length. Different from the results in calm water, both trajectories in this case are pushed away along the wave direction, but the ship still passes through the allowance region. The trajectory using the sliding mode controller drifts more away from the first waypoint than that using the PD controller. However, it gets better tracking in the following waypoints than the PD one does. Cost function values are listed in Table 3. Comparing with the results in Table 2, we find that it is more difficult to operate the ship in waves than in calm water because the costs in waves are significantly larger than those in calm water. Besides, considering the simulation time to reach the allowance region of the final waypoint using the same controller, we also find that it takes 510 s in calm water while it takes 528 s in regular waves. Therefore the wave effect on the ship operation can be seen and it indicates that sailing time and fuel consuming will increase due to wave effect. Motion responses in waves are shown in Figs. 6 and 7. In figures,  $\zeta_w$  presents the wave elevation at the ship's center of gravity. Because the following wave is set initially, the velocity ( $u$ ) of container ship is accelerated firstly then decelerated due to

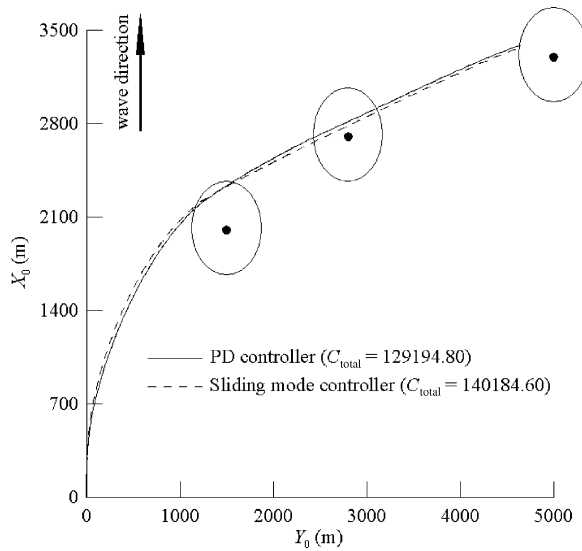


Fig. 5. The time domain simulation of ship trajectories in regular waves with  $\lambda/L=1$ ,  $a=1.5$  m.

additional resistances caused by the rudder deflection and other motions. In calm water case, the sway velocity and roll motion decrease with the decreasing rudder deflection, but they become periodic oscillations in waves because of the additional wave force and moment. The heave and pitch motions also become periodic due to the wave. In Fig. 5, it is not clear to observe the oscillation phenomenon on heading angle, but it is apparent as we can see from the time simulation records in Figs. 6 and 7. Because of the wave effect, the heading angle may not track well with the desired heading angle, then the controller must send commands to alter the rudder deflection to ensure the course is under control. Thus, the rudder deflection also appears to be oscillatory, and this phenomenon is distinct for sliding mode controller because its tracking ability is stronger than that of PD controller in this study.

In order to compare the efficiency of the two controllers, the case with the cost function value for sliding mode controller in Table 3, i.e. 140184.6, is selected to test for the PD controller. The new tuned parameters, yaw gain = 0.157 and yaw rate gain = 0.7, are tuned as possible to reach the corresponding cost function value after trial and error.

Table 3  
Cost function value (in regular waves)

	Cost due to heading error	Cost due to rudder deflection	Total cost
PD controller	61029.25	68265.55	129,294.80
Sliding mode controller	64544.95	75639.64	140,184.60

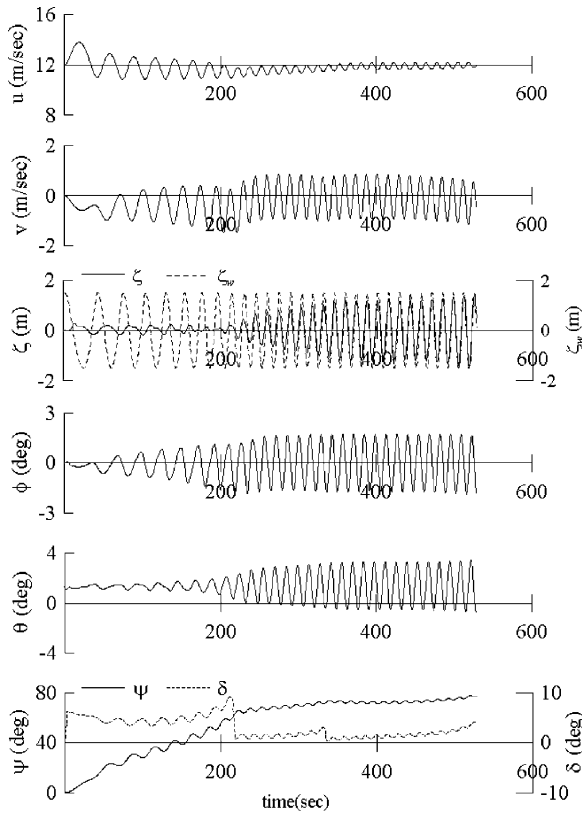


Fig. 6. The motion response for PD controller in regular waves with  $\lambda/L=1$ ,  $a=1.5$  m.

Fig. 8 presents a simulation result of PD controller with new tuned parameters and the comparisons with previous results are also shown. The new parameters lead to that the heading error cost, rudder deflection cost, and total cost are 71363.73, 68995.35 and 140,359.10, respectively. Comparing with the previous PD controller result, we find unsuitable parameters decrease the tracking ability and increase the rudder usage. These parameters will result in a poorer tracking trajectory. Even the cost of PD controller is tuned similarly to that of the sliding mode controller, its tracking ability is still worse according to the present investigation.

### 5. Conclusion

In this paper, a nonlinear hydrodynamic model with six degrees of freedom is successfully developed to investigate the course tracking ability of a ship steering in waves. The PD controller and the sliding mode controller are adopted and proper design

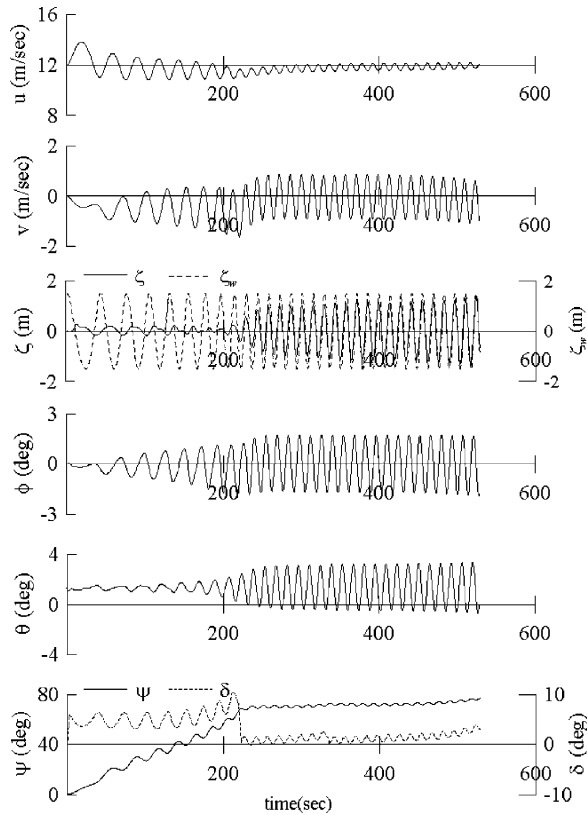


Fig. 7. The motion response for sliding mode controller in regular waves with  $\lambda/L=1$ ,  $a=1.5$  m.

parameters are tuned. From simulation results, both controllers are tracking well in calm water under the similar cost function value.

The wave effect on the operation of the ship autopilot is significant according to the comparison of the cost function values and the time consuming. Both controllers can conform to the course tracking command either in calm water or in regular waves. Although sliding mode controller is tracking well than PD controller in waves, its outcome leads to larger cost. However, even new parameters for PD controller are tuned to make the similar cost, the tracking effect is still worse than that using sliding mode controller according to the present case study.

The approximately optimal cost function value in this study is calculated by trial and error. In the future, it is recommended to apply the genetic algorithms to incorporate the present technique in the optimal control for ship autopilot.

The nonlinear hydrodynamic model with six degrees of freedom developed here is fairly rigorous because it can incorporate the existing controllers to predict the ship

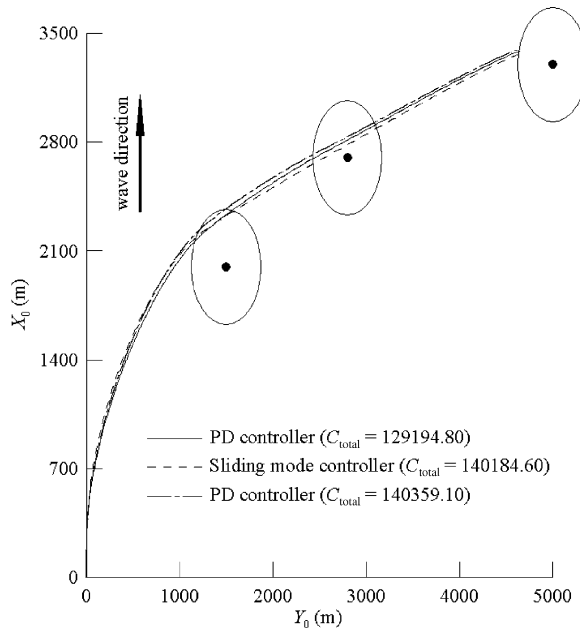


Fig. 8. The time domain simulation of ship trajectories in regular waves with  $\lambda/L=1$ ,  $a=1.5$  m.

trajectories in waves, even in random sea. It will be very helpful for naval architects while analyzing the ship maneuvering ability at sea.

## References

- Bailey, P.A., 1999. Maneuvering of a ship in a seaway. PhD Thesis, University of Southampton, UK.
- Fossen, T.I., 1994. Guidance and Control of Ocean Vehicles. Wiley, New York.
- Hamamoto, M., Kim, Y.S., 1993. A new coordinate system and the equations describing maneuvering motion of a ship in waves (in Japanese). *Journal of The Society of Naval Architects of Japan* 173, 209–220.
- Hamamoto, M., Matsuda, A., Ise, Y., 1994. Ship motion and the dangerous zone of a ship in severe following seas (in Japanese). *Journal of The Society of Naval Architects of Japan* 175, 69–78.
- Healey, A.J., Lienard, D., 1993. Multivariable sliding mode control for autonomous diving and steering of unmanned underwater vehicles. *IEEE Journal of Oceanic Engineering* 18 (3), 327–339.
- Hirano, M., 1980. On the calculation method of ship maneuvering motion at initial design phase (in Japanese). *Journal of The Society of Naval Architects of Japan* 147, 144–153.
- Hirano, M., Takashina, J., 1980. A calculation of ship turning motion taking coupling effect due to heel into consideration. *Transaction of the West-Japan Society of Naval Architects* 59, 71–81.
- Inoue, S., Hirano, M., Kijima, K., 1981a. Hydrodynamic derivatives on ship manoeuvring. *International Shipbuilding Progress* 28 (321), 112–125.
- Inoue, S., Hirano, M., Kijima, K., Takashina, J., 1981b. A practical calculation method of ship maneuvering motion. *International Shipbuilding Progress* 28 (325), 207–222.
- Kim, C.H., Chou, F.S., Tien, D., 1980. Motions and hydrodynamic of a ship advancing in oblique waves. *Transactions of the Society of Naval Architects and Marine Engineers* 88, 225–256.

- McGookin, E.W., Murray-Smith, D.J., Li, Y., Fossen, T.I., 2000a. Ship steering control system optimization using genetic algorithms. *Control Engineering Practice* 8, 429–443.
- McGookin, E.W., Murray-Smith, D.J., Li, Y., Fossen, T.I., 2000b. The optimization of a tanker autopilot control system using genetic algorithms. *Transactions of the Institute of Measurement and Control* 22, 141–178.
- Munif, A., Umeda, N., 2000. Modeling extreme roll motions and capsizing of a moderate-speed ship in astern waves. *Journal of the Society of Naval Architects of Japan* 187, 51–58.
- Nejim, S., 2000. Design of limited authority adaptive ship steering autopilots. *International Journal of Adaptive Control and Signal Processing* 14, 381–391.
- Slotine, J.J.E., Li, W., 1991. *Applied Nonlinear Control*. Prentice-Hall, New Jersey.
- Takahashi, T., 1969. Mechanism of rolling and application (in Japanese). Report of Mitsubishi Heavy Industry Nagasaki Technical Institute 1969, 2842.
- Tzeng, C.Y., Lin, K.F., 2000. Adaptive ship steering autopilot design with saturating and slew rate limiting actuator. *International Journal of Adaptive Control and Signal Processing* 14, 411–426.
- Umeda, N., Hashimoto, H., 2002. Qualitative aspects of nonlinear ship motions in following and quartering seas with high forward velocity. *Journal of Marine Science and Technology* 6, 111–121.
- Yoshimura, Y., Nomoto, K., 1978. Modeling of manoeuvring behavior of ships with a propeller idling, boosting and reversing (in Japanese). *Journal of the Society of Naval Architects of Japan* 144, 57–69.